

Application of Myco-Fabricated Silver Nanoparticle in the Adsorption of Malachite Green and Trypan Blue from Aqueous Solution

¹Okafor, Chioma Augusta, ¹Uba*, Bright Obidinma and ²Dokubo, Chinweike Unoma

¹Department of Microbiology, Chukwuemeka Odumegwu Ojukwu University, P.M.B.02 Uli, Anambra State, Nigeria.

²Department of Science and Laboratory Technology, Delta State Polytechnic Ogwashi – Uku, Nigeria

Correspondence: ubabright4real@yahoo.com; DOI: <https://doi.org/10.52417/njls.v12i2.354>

Abstract

The study was undertaken to assess the application of myco-fabricated silver nanoparticles in the adsorption of Malachite green and Trypan blue from an aqueous solution. The cell biomass suspensions of fungal endophytes isolated from the leaves of *Mannihot esculenta* and *Carica papaya* were used in the silver nanoparticles. The method involved in nanoparticles characterization, decolorization and adsorption treatment efficacy used UV-spectroscopy FT-IR, XRD and SEM, spectrophotometric analysis and phytotoxicity testing. The result revealed that the endophyte strains PDA 1 and PDA 2 were identified as *Aspergillus niger* and *Aspergillus fumigatus*. There was colour change from colourless to dark brown revealing the biogenic synthesis of silver nanoparticles due to the formation of clumps after 24 hr. The peaks observed in FT-IR spectra reflect the role of metabolites (functional groups) which act as capping and reducing agents. The UV-Vis spectral result showed the maximum peak of PDA 1 to be 620 nm at 0.933 absorbance while that of PDA 2 were 300 nm and 450 nm at 0.684 absorbance revealing the surface plasmon resonance. The XRD peaks of the nanoparticles were clearly distinguishable and broad indicating an ultra-fine nature. The microscopic characterization of PDA 1 and PDA 2 showed the presence of flake type, a smooth and irregularly shaped granulated compact powder with bright facets. The results of the decolorization profile showed that the adsorption efficiencies of both dyes were significantly concentration and time-dependent ($P < 0.05$). These findings suggest the potential of these nanoparticles in the environmental remediation of harmful dyes.

Keywords: Biosorption, Fungal endophyte, Malachite green, Silver nanoparticles, Trypan blue,

Introduction

Industrial pollution is a great concern for modern society and developing cyclic processes is one of the major challenges (Numan and Gokhan, 2020). Wastewater is a major environmental problem for the growth of the textile industry besides other issues like solid waste and hazardous waste management. Textile and dye industries use various kinds of synthetic dyes and at the same time discharge large amounts of highly textile wastewater into the environment. This highly coloured textile wastewater severely affects receiving environments. This situation also has an impact on biological life due to low oxygen consumption and light penetration. It may also be dangerous to certain forms of aquatic life due to the occurrence of component metals and chlorine present in the synthetic dyes of textile wastewater (Numan and Gokhan, 2020). So, there is a conclusive need for the destruction of this hazardous waste from industrial effluents before disposal to the environment. In the past few years, nanomaterials have attracted good attention due to their exceptional physical, chemical, and biological properties, which led to them having many applications in different fields, e.g., biomedicine, drug delivery, optics, environment, catalysis, food industry, agriculture, and water treatment (Khalil *et al.*, 2013). Recently, the biogenic (green chemistry) metal nanoparticle (NP) synthesis method that employs biological entities, such as microorganisms and plant extracts, has been suggested as a valuable alternative to other synthesis routes. It is known that microorganisms, such as bacteria and fungi, play a vital role in remediation of toxic materials by reducing metal ions. The mechanism of silver nanoparticles synthesis using fungi involved the following steps: 1. trapping of Ag ions at the surface of the fungal cells 2. reduction of the adsorbed silver ions by the enzymes

present with the fungal system (Rajput *et al.*, 2017). The green synthesis of AgNPs with naturally occurring reducing agents could be a promising method to replace more complex physiochemical syntheses since the green synthesis is free from toxic chemicals and hazardous byproducts and instead involved natural capping agents for the stabilization of AgNPs (Lee and Jun, 2019). Therefore, microbially synthesized nanoparticles have been shown to be safe, easy and economical in wastewater treatment in addition to being effective in environmental applications.

There are several literatures containing reports of fungal endophytes having great potential to secrete structurally diversified metabolites (Baker and Satish, 2012; Azmath *et al.*, 2016; Rajput *et al.*, 2017). But one of the least studied areas in the field of endophytes is their evaluation for nanoparticle synthesis (Azmath *et al.*, 2016). The interference of fungal endophytes with nanoparticles is relatively new and is expected to have significant impact in the course of time. Also, there are limited and paucity of information regarding their applicability in the adsorption and subsequently decolorization of dyes and therefore form the thrust of this study. This study was undertaken to examine the application of myco-fabricated silver nanoparticles in the adsorption of malachite green and trypan blue from aqueous solution.

Materials and Methods

Description of Specimen Site

The specimens were located at the female hostel of Chukwuemeka Odumegwu Ojukwu University Uli Campus, Anambra State. The coordinates of the sampling points Latitude 05° 46'18.56" and Longitude 06° 50'16.09" and it's elevation is 64 m were recorded using Global Positioning System (GPS) App was shown in Plate 1.

The area had rainfall seasons from April to October and human activities.

Specimen Collection

The *Carica papaya* and *Mannihot esculenta* leaves were harvested using a sharp knife, placed in a sterile polyethylene bag and were immediately transported to Microbiology Postgraduate Laboratory, Chukwuemeka Odumegwu Ojukwu University, Umuoma Uli, Campus, Anambra State, Nigeria.



Plate 1: High resolution satellite image showing the location of cassava and paw paw leave collection point. Source: Ezeomodo (2022)

Isolation of Fungal Endophyte

By adopting the modified method of Marchut-Mikolajczyk *et al.* (2010), the following surface sterilization conditions were applied: 70 % ethanol for 3 min, 1 % sodium hypochlorite for 12 min and 70 % ethanol for 30 s. After the final ethanol step, the plant parts were rinsed five times with sterile distilled water. Surface-sterile plant samples were cut with a sterile scalpel into small pieces (~1 cm) under sterile conditions and placed on the sterile Potato Dextrose Agar media (PDA). The efficiency of the sterilization process was verified by pipetting 100 μ L of water from the last wash onto PDB medium and monitoring possible microbial growth.

Source of Organism and Characterization

Two fungal strains were selected based on distinct morphological features. Individual fungal colonies were picked and further purified by subculturing on PDA and incubated at 28 °C. The identification of the isolates was carried out using colonial, and microscopic techniques (Moustafa, 2017).

Colonial and microscopic morphological technique

The fungal morphology was studied macroscopically by observing the colony features (colour, shape, size and hyphae), and microscopically by a compound microscope with lactophenol cotton blue stained slide mounted with a small portion of the mycelium (Alsohaili and Bani-Hassan, 2018).

Preparation of the Supernatant

For fungal biomass preparation, the selected two fungal cultures were grown in the liquid medium containing (g/l): KH_2PO_4 7.0; K_2HPO_4 2.0; $\text{MgSO}_4 \cdot 7\text{H}_2\text{O}$ 0.1; $(\text{NH}_4)_2\text{SO}_4$ 1.0; yeast extract 0.6 and glucose 10.0. Flask containing medium was incubated for 7 days at 28 ± 2 °C. After the incubation, the biomass was harvested through centrifugation at 4000 rpm for 25 min and washed with distilled water. Thereafter, the biomass was added to 100 mL of deionized water and further incubated for 72 hr. After the incubation, the fungal filtrate was obtained by passing the suspension through Whatman No. 1 filter paper and the filtrate recovered (Moustafa, 2017).

Preparation of Silver Nitrate Solution

An accurate concentration of 5 mM silver nitrate (AgNO_3) was prepared by dissolving 0.081 g of AgNO_3 in 100 mL of double sterile distilled water and stored in amber coloured bottle to prevent auto oxidation of silver (Moustafa, 2017).

Synthesis of Silver Nanoparticles

Silver nanoparticles were synthesized by drop-wise addition of 50 mL of both fungal cell filtrate into a 250 mL Erlenmeyer flask containing 50 mL of AgNO_3 solution and heated with magnetic stirrer at 70 °C for 24 hr until the formation of dark brown colour of silver nanoparticles was observed. Afterwards, the synthesized AgNO_3 were washed using 70 % ethanol and sterile water in a centrifuge (Sundaram and Ramasamy, 2015).

Characterization of the Synthesized Silver Nanoparticles (AgNPs)

The produced AgNPs were characterized by visible colour change determination, UV-Visible spectroscopy at wavelengths ranging from 200 - 800 nm. The phase purity and crystalline nature was determined by X - ray Diffractometer. The size and morphologies of the formed NPs were determined by using scanning electron microscopy (SEM). The functional groups of produced AgNPs were determined using the Fourier transform infrared (FTIR) spectroscopy at Springboard Research Laboratory Awka, Anambra State Nigeria (Wang *et al.* 2014; Fazlzadeh *et al.* 2016; Moustafa, 2017).

Batch Experiment on Dye Decolourization

Decolorization of malachite green and trypan blue experiments was carried out at room temperature and at its original pH according to the method of Sravanthi *et al.* (2018). In this study, the sorbent materials (nanoparticles) were mixed with 500 mL aqueous solutions of malachite green and trypan blue solutions at different concentrations (50 - 400 ppm). The mixture was stirred for a certain period of time (0, 1, 2, 10, and 24 hr) using a magnetic stirrer to find out the effect of contact time on the removal of malachite green and trypan blue. During the adsorption process, about 5 mL of aliquot samples was withdrawn from the reaction mixture by syringe at time intervals above and the sorbent was removed using 0.45 µm filters. The concentrations of Malachite green and Trypan blue, remaining in solution, was determined spectrophotometrically at absorbances of 624 and 580 nm, respectively. The change in the concentration of malachite green and trypan blue was calculated from the difference between the initial and final equilibrium concentrations of malachite green and trypan blue, and sorption efficiency or removal efficiency of the sorbent was computed from the following equation 1 below:

$$\text{Percentage removal (\%)} = \frac{C_0 - C_e}{C_0} \times 100 \quad \text{Eqn 1.}$$

where C_0 and C_e are total dissolved and equilibrium liquid phase concentrations (mg L⁻¹) respectively. The amount of adsorbate adsorbed on the surface of sorbent at equilibrium (q_e) (mg/g) was calculated in equation 2 as:

$$q_e = \frac{(C_0 - C_e) v}{m} \quad \text{Eqn 2.}$$

where v (in litre) is the volume amount of adsorbent.

Phytotoxicity Evaluation

The method of Selim *et al.* (2012) was adopted with slight modification, using the seed germination technique. A monocotyledonous plant maize seeds (*Zea mays*) and dicotyledonous plant bean seed (*Phaseolus vulgaris*) were surface sterilized by immersion in 75 % ethanol for 3 min followed by transferring in 0.001 % HgCl₂ solution for 2 min with periodical agitation and finally thoroughly washed with sterilized distilled water to get rid of toxic chemicals. Ten millilitres of the sterile distilled water as well as the treated test filtrates were applied to filter paper in Petri dishes. Also, 10 sterile seeds of each plant were then placed on the filter paper. All experiments were run in triplicate. The Petri dishes were sealed with tape to minimize water loss while allowing air penetration and then incubated in the dark for 120 hr at room

temperature. The seed germination in distilled water plates without treated test filtrates served as control. The germination index (GI) was calculated after 120 hr incubation as follows:

$$\text{Germination index (\%)} = \frac{\text{Seed Germination (\%)} \times \text{Root elongation (\%)}}{100} \quad \text{Eqn 3.}$$

Statistical Analysis

The data were subjected to descriptive statistics and mean ± standard deviations. The mean values were subjected to two - way analysis of variation (ANOVA) followed by Tukey's multiple comparison test using GraphPad Prism Software version 9.3.1 (San Diego, USA). The obtained values less than 0.05 were considered significant at 95 % confidence intervals.

Results

The results of the cultural and microscopic features of the fungal isolate are presented in Table 1, respectively. From the table, the PDA 1 isolate showed a deep brown colony, with smooth wall and surface, rapid growth and reverse uncoloured. Microscopically, the spore is sporangiophore, long non-septate hollow hypha with sporangiospore borne in sporangium which was identified tentatively as *Aspergillus niger*. In PDA 2 isolate, there was presence of grey colony, smooth walled and surface, raised, downy texture, rapid growth and reversed pale. Microscopically, it has conidia with short septate hyphae and possesses spores that are distributed along the hypha walls which was tentatively identified as *Aspergillus fumigatus*. The synthesis of AgNPs was carried out

using filtrates combinations of PDA 1 and PDA 2 isolates in a hot magnetic stirrer at 70 °C for 24 hr. It was observed that the AgNO₃ changed from colourless to brownish then to dark brown signifying nanoparticles formations. Fourier Transform- Infra red (FT-IR) spectral peaks of the green synthesized nanoparticle are shown in Figure 1. From the figure, peak 825.145 cm⁻¹ corresponds to para-Di substitution vibration due to = C - H bend aromatic group. Peak at 1290.859 cm⁻¹ corresponds C-O vibration due to carboxylic acid group. Peaks at 1428.91 corresponds to variably strong C - O stretching vibration due to ester group. Peaks at 1628.335 cm⁻¹ corresponds to variably strong N - H bend stretching vibration due to amide group. Peaks between 1826.354 corresponds to strong C = O stretching vibration due to acid anhydride group. Peak 2027.12 cm⁻¹ corresponds to strong asymmetric N=C=S stretching vibration due to thiocyanate ion group. The peaks between 2136.477 cm⁻¹ and 2193.54 cm⁻¹ corresponds to variable C≡C stretching vibration, dialkyl compounds due to disubstituted alkynes group. Peaks between 2454.509 cm⁻¹ and 3453.001 cm⁻¹ corresponds to strong, broad hydrogen bond O-H stretching vibration due to carboxylic acid group. Peaks between 3549.507 cm⁻¹ and 3810.117 cm⁻¹ corresponds to variable O-H stretching vibration due to alcohol and phenol groups. The result of the UV- vis spectral profile of synthesized AgNPs is shown in Figure 2. From the figure, the synthesized nanoparticle had maximum peak of 0.684 absorbances at 330 nm and 450 nm wavelengths as well as the lowest peak of 0.032 absorbances at 870 nm wavelength, respectively. The results of the phase purity and crystalline characteristics of the biosynthesized silver nanoparticles is

demonstrated in Table 2 and Figures 3. From the results, the XRD peaks of nanoparticles was clearly distinguishable and broad indicating an ultra-fine nature. From the Table 2 and Figure 3, the XRD spectrum of the synthesized AgNPs showed five characteristic intense peaks at $2\theta = 33.16, 34.20, 38.02, 44.19$ and 64.49 corresponds to hkl of (100, 100, 110, 111 and 220, respectively) planes of centered cubic silver. Figure 4 showed the scanning electron microscopy image of the green silver nanoparticle. The Figure showed the presence of dispersed flake type, irregular shaped and a smooth granulated compact powder with brighter facets.

Figures 5 and 7 showed the effect of contact time on percentage removal efficiency with respect to different concentrations of myco-synthesized silver nanoparticle on malachite green and trypan blue dye, respectively. From the Figure 5 result, 50 mg/L and 400 mg/L of myco-synthesized silver nanoparticle had the lowest (15.1 %) and highest (90.4 %) percentage removal efficiency of malachite green dye at 0 and 24 hr while from the Figure 7 result, 50 mg/L and 400 mg/L of myco-synthesized silver nanoparticle had the lowest (13.9 %) and highest (85.0 %) percentage removal efficiency of trypan blue dye at 0 and 24 hr, respectively. Statistically, there were significant ($p < 0.05$) differences detected among the means of treatment concentration/dosage and contact time of dye adsorption reaction. Figures 6 and 8 showed the effect of contact time on unit removal capacity with respect to different concentrations of myco - synthesized silver nanoparticles on

malachite green and trypan blue dyes, respectively. From the Figure 6 result, 100 mg/L and 50 mg/L of myco-synthesized silver nanoparticle had the lowest (1.96 mg/g) and highest (12.52 mg/g) unit removal capacity of malachite green dye at 0 and 24 hr while from the Figure 8 result, 400 mg/L and 50 mg/L of myco-synthesized silver nanoparticle had the lowest (3.10 mg/g) and highest (18.86 mg/g) unit removal capacity of trypan blue dye at 0, 1 and 24 hr, respectively. Statistically, there were significant ($p < 0.05$) differences detected among the means of treatment concentration/dosage and contact time of dye adsorption reaction.

The result of the germination index of *Z. mays* and *P. vulgaris* seeds when exposed to decolourized malachite green and trypan blue dye with biosynthesized silver nanoparticle after 24 hr treatment is shown in Figure 9. From the figure, concentration 0.025 g of malachite green decolourized sample had the highest germination index (34.1 %) while 0.2 g had the lowest germination index (11.3 %) in *Zea mays* seeds, respectively. Also, concentration 0.025 g of malachite green decolourized sample had the highest germination index (57.1 %) while 0.2 g had the lowest germination index (22.8 %) in *P. vulgaris* seeds, respectively. Similarly, concentration 0.05 g of trypan blue decolourized sample had the highest germination index (70.5 %) while 0.1 g lowest germination index (41 %) in *Zea mays* seeds, respectively. Also, concentration 0.1 g trypan blue decolourized sample had the highest germination index (81.4 %) while 0.15 g had the lowest germination index (11.4 %) in *P. vulgaris* seeds, respectively.

Table 1: Cultural and microscopic features of the two fungal isolates

Isolate code	Cultural character	Microscopic character	Identity
PDA 1	Deep brown colony, downy texture, smooth walled and surface, rapid growth, reverse uncoloured.	The spore is sporangiophore, the hyphae is hollow that, is, non-septate hypha with sporangiospore borne in sporangium, the hyphae is longer.	<i>Aspergillus niger</i>
PDA 2	Grey colony, smooth walled and surface, raised, downy texture, rapid growth, reverse pale.	It has conidia with short septate hyphae and the spores are distributed along the hypha walls	<i>Aspergillus fumigatus</i>

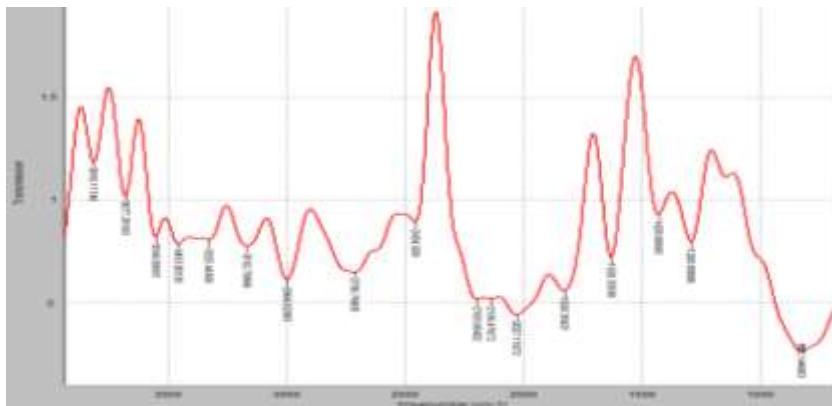


Fig. 1: FTIR spectral profile of green silver nanoparticle

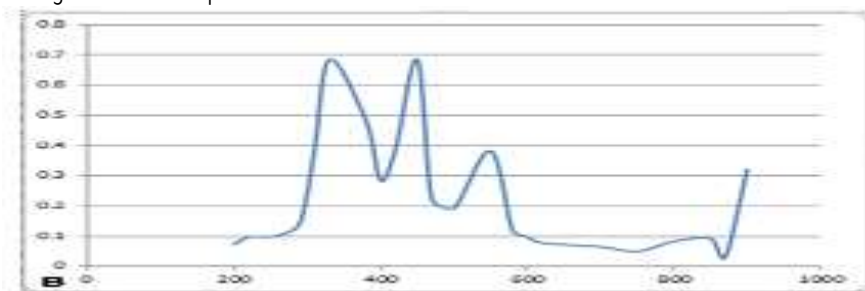


Fig. 2: UV-VIS spectral profile of biosynthesized silver nanoparticle

Table 2: Phase purity and crystalline characteristics of the green synthesized silver nano particles

Synthesized AgNPs	Peak no.	2 Θ	Cos Θ	Sin Θ	FWHM	β radian	Crystalline size 'D' nm	Hkl identified from peak
PDA 1 and 2	1	33.16			0.1968	0.0034	42.01	100
			0.9584	0.2853				
	2	34.20	0.9557	0.2940	0.1574	0.0027	53.32	100
	3	38.02	0.9454	0.3257	0.1968	0.0034	43.32	110
	4	44.19	0.9265	0.3762	0.0984	0.0017	86.65	111
	5	64.49	0.8457	0.5335	0.1181	0.0020	81.56	220

N.B: AgNPs = Silver nanoparticles; Θ = Theta; FWHM= full width at half maximum; β = Beta; hkl= integers representing lattice planes.

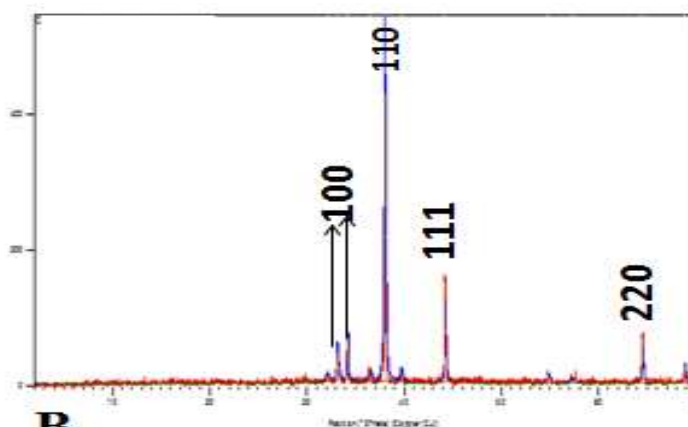


Fig. 3: XRD profile pattern of the biosynthesized AgNPs

N.B: XRD= X-ray diffraction; AgNPs= Silver nanoparticles

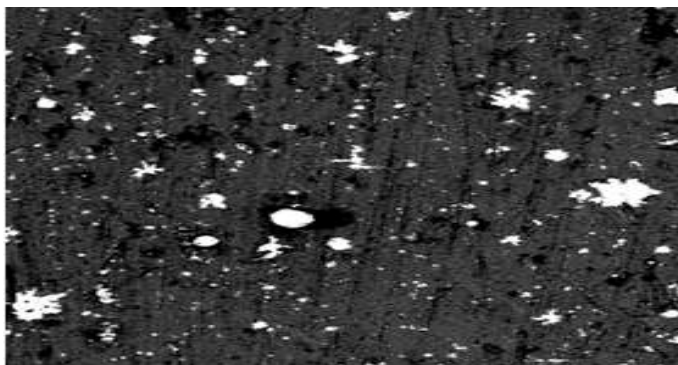


Fig. 4: Scanning electron microscope image (500x) of the synthesized AgNPs
 N.B: AgNPs= Silver nanoparticles

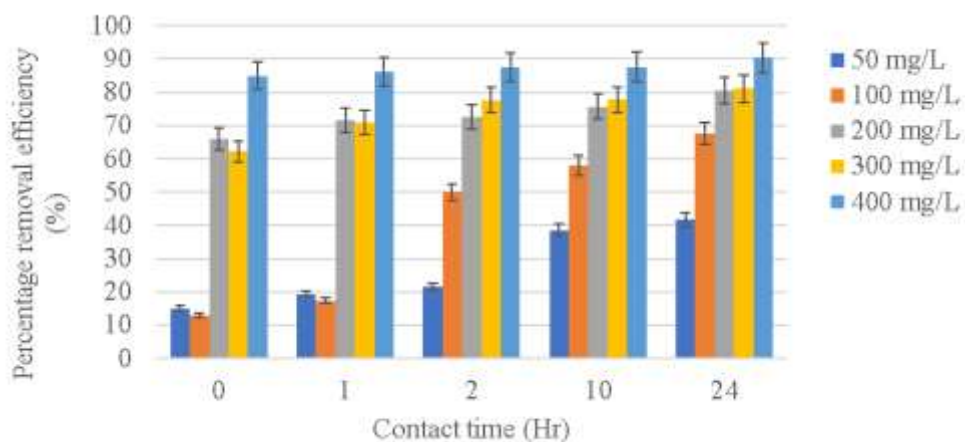


Fig. 5: Effect of contact time on percentage removal efficiency with respect to different concentrations of myco-synthesized silver nanoparticle on Malachite green dye
 Key: % = Percentage; mg/L = Milligram per litre; Hr = Hour; Error bar = Standard deviation

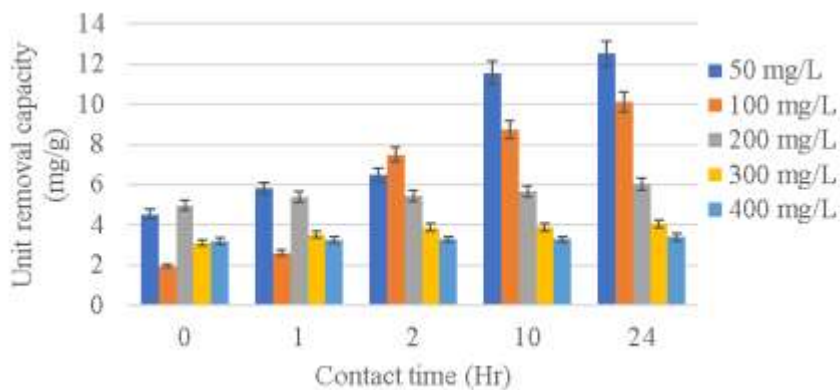


Fig. 6: Effect of contact time on unit removal capacity with respect to different concentrations of myco-synthesized silver nanoparticle on Malachite green dye
 Key: mg/g = Milligram per gram; mg/L = Milligram per litre; Hr = Hour; Error bar = Standard deviation

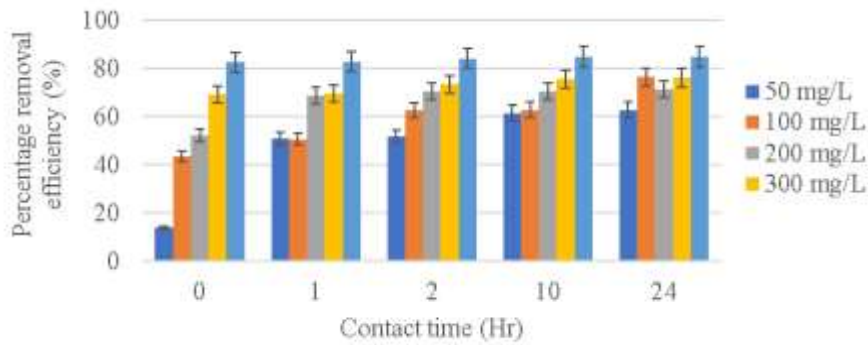


Fig. 7: Effect of contact time on percentage removal efficiency with respect to different concentrations of myco-synthesized silver nanoparticle on Trypan blue dye
Key: % = Percentage; mg/L = Milligram per litre; Hr = Hour; Error bar = Standard deviation

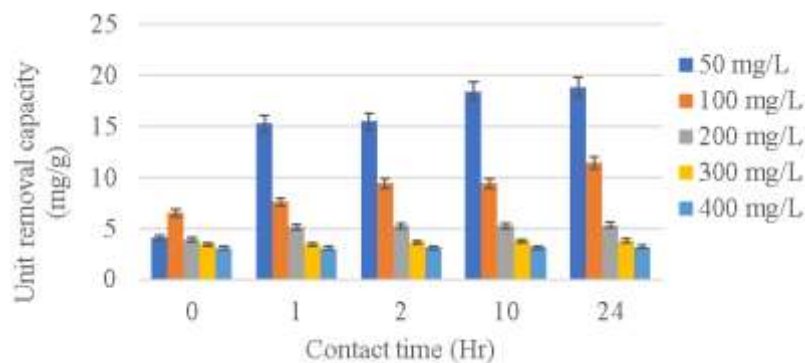


Fig. 8: Effect of contact time on unit removal capacity with respect to different concentrations of myco-synthesized silver nanoparticle on Trypan blue dye
Key: mg/g = Milligram per gram; mg/L = Milligram per litre; Hr = Hour; Error bar = Standard deviation

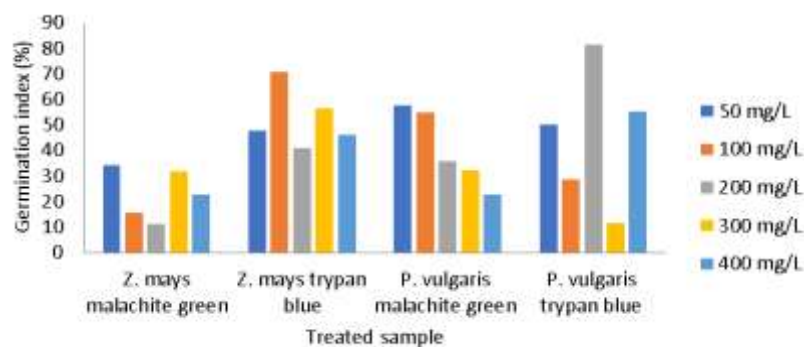


Fig. 9: Germination index of *Z. mays* and *P. vulgaris* seed when exposed to decolorized Malachite green and Trypan blue dye with biosynthesized silver nanoparticle after 24 hr treatment
N:B: % = Percentage, g = Gram

Discussion

Industrial pollution is a great concern for modern society and development cyclic processes is one of the biggest challenges. Wastewater is a major environmental problem for the growth of the textile industry besides other issues like solid waste and hazardous waste management. In this study, the application of myco-fabricated silver nanoparticles in the adsorption of malachite green and trypan

blue from aqueous solution was evaluated. Based on morphological and culturable characteristics, the two fungal strains of PDA 1 and PDA 2 were studied and the organisms' identified showed that PDA 1 was *Aspergillus niger*, and PDA 2 was *Aspergillus fumigatus* as represented in Tables 1 and 2, respectively. The myco-synthesis of metals and metal oxide NPs has recently drawn more attention due to high scalability, easy handling, high metabolite secretions. Moreover, fungi are characterized by high accumulation and high

tolerance to metal, as well as high biomass production that is used to produce high active metabolites. Many investigators have reported the potentials of endophytic fungal species such as *Aspergillus*, *Penicillium*, *Fusarium*, *Trichoderma* and *Pestalotiopsis* in the synthesis of nanoparticles (Rajput *et al.*, 2017; Verma *et al.* 2010).

In this study, the combined biomass filtrates of *A. niger* and *A. fumigatus* were utilized as biocatalyst for the green synthesis of AgNPs. The first monitor for successful fabrication was the colour change of fungal biomass filtrate from colourless to dark. Changing of the colour indicated the activity of metabolites involved in biomass filtrates. The colour change could also be due to the excitation of Surface Plasmon Resonance (SPR) of the synthesized AgNPs (Anjana and Geetha, 2019). The bioactive compounds present in biomass filtrates of *A. niger* and *A. fumigatus*, as previously described in the results section above are responsible for the reduction of metal precursors to form AgNPs are identified by FTIR as shown in Figure 1. The successful fabrication of AgNPs was confirmed by the peaks observed at the wave number 400 to 700 cm^{-1} , as reported in various published studies. The peaks observed in FT-IR spectra reflect the role of metabolites involved in biomass filtration of *A. niger* and *A. fumigatus* for reducing and stabilizing of AgNPs. These results obtained corroborate the findings of previous scientific literatures which clearly suggest the metabolic diversity of the fungal communities responsible for mediating the synthesis of the silver nanoparticles. Earlier FTIR analysis revealed the role of biomolecules which reduced the silver nitrate and bound onto the nanoparticles to stabilize them and prevent aggregation (Azmath *et al.*, 2016).

In order to further confirm AgNPs formation, the colour change was evaluated by UV-Vis spectroscopy to detect the maximum surface plasmon resonance (SPR). The size, shape and well distribution of the green synthesized NPs were usually influenced by SPR as reported previously by Fedlheim and Foss (2001). In this regard, Jeevanandam *et al.* (2018) reported that the size of biosynthesized AgNPs tends to be small when the SPR is less than 300 nm, whereas it becomes more anisotropic at SPR greater than 300 nm. In this present study, Figure 2 revealed that the maximum absorption wavelengths for the myco-synthesized silver nanoparticles ranged from 330 – 450 nm. The absorption peak of silver nanoparticles as reported in many studies ranged from 400 – 450 nm and is in line with the observation made in this study (Rajput *et al.*, 2017). Therefore, we can assume the efficacy of secondary metabolites involved in biomass filtrate to reduce, cap and stabilize AgNPs.

The crystalline nature of myco-synthesized AgNPs was investigated using XRD analysis. From Figure 3, the XRD peaks confirmed the phase purity and crystallographic structure of the myco-synthesized AgNPs. The results obtained in this study is in agreement with the published work of Azmath *et al.* (2016) who reported that the crystalline nature of the synthesized silver nanoparticles depicted with Bragg's peak 38.2°, 44.42°, 64.5°, 77.4° corresponding to the cubic facets of the particles and justifies the standard diffraction pattern of silver nanoparticles. The crystal size of myco-synthesized AgNPs was obtained as 50 nm from the

XRD pattern by the Debye-Scherrer equation. Anjana and Geetha (2019) reported that the average size of the AgNPs synthesized was approximate to be ~13 nm which is obtained using similar formula. The reported sizes of these particles ranged between 5 – 50 nm (Rajput *et al.*, 2017). The surface morphology of myco-synthesized AgNPs, agglomeration and qualitative and quantitative chemical compositions were investigated using SEM. The result in Figure 4 is in line with previous studies on myco-synthesis of silver nanoparticles using *Aspergillus*, *Penicillium*, *Fusarium* and *Pleurotus* species (Rajput *et al.*, 2017).

After properly characterizing our test samples, we performed the bioadsorption study to investigate the proficiency of the myco-synthesized AgNPs in aqueous dye solution treatments. The results in Figures 5 – 8 displayed that Malachite green and Trypan blue removal efficiencies remarkably increased upon enhancing the Ag NPs dosages (50 – 400 mg) at increasing time (0 – 24 hr), which might be rationalized by the larger accessible specific areas and more unsaturated sites for sorption. On the other hand, dye molecules absorbed on the surface of myco-synthesized AgNPs will act as an electrophilic agent and capture the electron available on the surface of myco-synthesized AgNPs. This overall process starts a relay of dye degradation reaction and breaks the dye molecule into a colourless component. Comparatively, there was faster and higher rates of malachite green dye adsorption than trypan blue dye adsorption. Statistically, there were significant ($p < 0.05$) differences detected among the means of treatment concentration/dosage and contact time of dye adsorption reaction. The results of this study suggest that potentially competent myco-synthesized silver nanoparticles can be efficiently used for detoxification and bioremediation of harmful dyes and textile effluents which is in conformity with the observations of Rajput *et al.* (2017). A similar increase in degradation rate for the other dyes such as methylene blue, congo red, thymol blue, methyl orange, safranin, crystal violet, rhodamine B dye, Orange G et cetra was observed, reported and documented by several researchers (Anjana and Geetha, 2019; Moghadad *et al.* 2020; Albeladi *et al.* 2020; Kaushik *et al.* 2021).

In order to explore the success of the bioadsorption treatment, germination index which combined measures of relative seed germination and relative root growth, was used to evaluate the toxicity of the biosurfactant to the seeds of *Zea mays* and *P. vulgaris*. The results in Figure 9 revealed that the treated solutions tested had no inhibitory effect on seed germination or root growth indicating low toxicity of the malachite green and trypan blue decolorized samples, as the leaf growth and growth of secondary roots were evident under all the tested concentrations. Similar observation was obtained by Rani *et al.* (2014) who demonstrated that seed germination examination to show the effect of untreated and treated dyes on germination of wheat seeds. They reported that germination percentage was higher up to 90 % by treated dye, while the untreated (control) dye inhibited the germination of wheat seeds even after four days of observation.

Conclusion

In this study, the green and novel synthesis of AgNPs in an eco – friendly manner by fungal biomass extracts was reported. The colour change of the synthesized AgNPs from colourless to dark brown confirmed the successful synthesis which was further validated by FTIR, UV-Vis spectroscopy, XRD analysis and SEM results. The catalytic efficiency of the myco - synthesized silver nanoparticles during the decolorization of the malachite green dye was found to be higher and faster than trypan blue dye as well as statistically significant ($P < 0.05$). The phytotoxicity carried out in this research was found to be non – inhibitory to the seeds of *Zea mays* and *P. vulgaris*, respectively demonstrating the potentials of these particles in the treatment of textile and dangerous effluents and dyes in either aquatic or terrestrial ecosystems.

References

- Albeladi, S. S. R., Malik, M. A. & Al-Thabaiti, S. A. (2020). Facile biofabrication of silver nanoparticles using salvia officinalis leaf extract and its catalytic activity towards congo red dye degradation. *Journal of Material Research and Technology*, 9: 10031 – 10044.
- Alsohaili, A. S. & Bani-Hasan, M. B. (2018) Morphological and molecular identification of fungi isolated from different environmental sources in the northern eastern desert of Jordan. *Journal of Biological Science*, 329 – 337
- Anjana, R. & Geetha, N. (2019). Degradation of methylene blue using silver nanoparticles synthesized from *Cynodon dactylon* (L.) Pers. leaf aqueous extract. *International Journal of Scientific and Technology Research*, 8 (9): 225 – 229.
- Azmah, P., Baker, S., Rakshith, D. & Satish, S. (2016). Myco - synthesis of silver nanoparticles bearing antibacterial activity. *Saudi Pharmaceutical Journal*, 25 (1): 140 – 146.
- Baker, S. & Satish, S. (2012). Antimicrobial activity and biosynthesis of nanoparticles by endophytic bacterium inhabiting Coffee arabica. L. *Scientific Journal of Biological Science* 1, 107– 113.
- Fazlzadeh, M., Rahmani, K., Zarei, A., Abdoallahzadeh, H., Nasiri, F. & Khosravi, R. (2016). A novel green synthesis of zero valent iron nanoparticles (NZVI) using three plant extracts and their efficient application for removal of Cr (VI) from aqueous solutions. *Advanced Powder Technology*, Article in Press: <http://dx.doi.org/10.1016/j.apt.2016.09.003>.
- Khalil, K. A., Fouad, H., Elsnagawy, T. & Almajhdi, F. N. (2013). Preparation and characterization of electrospun PLGA/silver composite nanofibers for biomedical applications. *International Journal of Electrochemical Science*, 8: 3483 – 3493.
- Kaushik, A., Gola, D., Raghav, J., Gupta, D., Kumar, A., Agarwal, M., Chauhan, N., Srivastava, S.K. & Tyagi, P.K. (2021). Synthesis of silver nanoparticles using egg white: dye degradation and antimicrobial potential. *Biointerface Research Research in Applied Chemistry*, 12 (2): 2361 – 2372.
- Lee, S. H. & Jun, B. H. (2019). Silver nanoparticles: synthesis and application for nanomedicine. *International Journal of Molecular Sciences*, 20 (4): 865. <https://doi.org/10.3390/ijms20040865>.
- Marchut-Mikolajczyk, O., Piotr, D., Dominika, P. & Tadeusz, A. (2018). Biosurfactant production and hydrocarbon activity of endophytic bacteria isolated from *Chelidonium majus* L. *Microbial Cell Factories*, 17:171
- Moghadas, M.R.S., Motamedi, E., Nasiri, J., Naghavi, M.R. & Sabokdast, M. (2020). Proficient dye removal from water using biogenic silver nanoparticles prepared through solid-state synthetic route. *Heliyon*, 6: e04730.
- Moustapha, M. T. (2017). Removal of pathogenic bacterial from wastewater using silver nanoparticles synthesized by two fungal species. *Water Science*, 31: 164 – 176
- Numan, Y. & Gokhan, O. E. (2020). Agar-plate screening for textile wastewater decolorization by Some White rot Fungi. *EC Microbiology*, 16 (9): 20 – 24.
- Rani, B., Kumar, V., Singh, J., Bisht, S., Teotia, P., Sharma, S. & Kela, R. (2014). Bioremediation of dyes by fungi isolated from contaminated dye effluent sites for bio-usability. *Brazilian Journal of Microbiology*, 45 (3): 1055 – 1063.
- Rajput, K., Agrawal, S., Sharma, J. & Agrawal, P. (2017). Mycosynthesis of silver nanoparticles using endophytic fungus and investigation of its antibacterial and azo dye degradation efficacy *Pestalotiopsis versicolor*. KAVAKA, 49:65 – 71.
- Selim, S. M., Zayed, M. S. & Atta, H. M. (2012). Evaluation of phytotoxicity of compost during composting process. *Nature and Science Material*. 10: 69 – 77.
- Sravanthi, K., Ayodhya, D. & Swamy, P.Y. (2018). Synthesis, characterization of biomaterial-supported zero-valent iron nanoparticles for contaminated water treatment. *Journal of Analytical Science and Technology*, 9:3. DOI 10.1186/s40543-017-0134-9.
- Sundaram, J. & Ramasamy, H. (2015). Biosynthesis of silver nanoparticles using soil fungi. *Journal of Engineering Science Resource Technology*, 24 (2).
- Verma, V. C., Gond, S. K., Kumar, A., Kharwar, R. N., Boulanger, L. A. & Strobel, G. A. (2011). Endophytic fungal flora from roots and fruits of an Indian neem plant *Azadirachta indica* A. juss., and impact of culture media on their isolation. *Indian Journal of Microbiology* 51: 469 – 476.
- Wang, T., Jin, X., Chen, Z., Megharaj, M. & Naidu, R. (2014a). Green synthesis of Fe nanoparticles using eucalyptus leaf extracts for treatment of eutrophic wastewater. *Science Total Environment* 210:466 – 467.